A rate and state friction law for saline ice

A rate and state friction law for saline ice

Ben Lishman,[1] Peter Sammonds,[1,2] and Danny Feltham[2,3]

Received 13 April 2010; revised 23 October 2010; accepted 26 January 2011; published 19 May 2011.

[1] Sea ice friction models are necessary to predict the nature of interactions between sea ice floes. These interactions are of interest on a range of scales, for example, to predict loads on engineering structures in icy waters or to understand the basin-scale motion of sea ice. Many models use Amonton's friction law due to its simplicity. More advanced models allow for hydrodynamic lubrication and refreezing of asperities; however, modeling these processes leads to greatly increased complexity. In this paper we propose, by analogy with rock physics, that a rate- and state-dependent friction law allows us to incorporate memory (and thus the effects of lubrication and bonding) into ice friction models without a great increase in complexity. We support this proposal with experimental data on both the laboratory (~0.1 m) and ice tank (~1 m) scale. These experiments show that the effects of static contact under normal load can be incorporated into a friction model. We find the parameters for a first-order rate and state model to be $A = 0.310$, $B = 0.382$, and $\mu_0 = 0.872$. Such a model then allows us to make predictions about the nature of memory effects in moving ice-ice contacts.

Citation: Lishman, B., P. Sammonds, and D. Feltham (2011), A rate and state friction law for saline ice, *J. Geophys. Res.*, *116*, C05011, doi:10.1029/2010JC006334.

1. Introduction

[2] Improved modeling of sea ice friction may be important in several fields. On an engineering scale, ice-ice friction modeling allows the prediction of ice stresses and hence loads on offshore structures [e.g., *Hopkins et al.*, 1991]. On a larger scale, discrete element models of sea ice behavior help to inform sea ice climate model design and tuning [*Wilchinsky et al.*, 2006], and these discrete element models suggest in-plane sliding (and hence frictional modeling) is crucial to our understanding of basic-scale processes. *Weiss et al.* [2007] demonstrate that Arctic sea ice deformation is characterized by nonequilibrium dynamics, and that dynamic friction across scales governs the deformation. Observations from *Kwok* [2001] suggest that overall Arctic sea ice behavior is governed by a few large shear zones; an improved model of friction, applied to these faults, could lead to new insights into the overall behavior of the Arctic.

[3] Sliding between sea ice floes is opposed by friction. The energy dissipated by this frictional sliding heats the floes, which may cause melting on the sliding interface, and hence lubrication and a decrease in friction. If the local temperature is below the freezing point of seawater, asperities may freeze together. These freeze bonds then have to be ruptured, increasing the force required to move the floes relative to each other, and hence increasing the effective friction coefficient. The balance between friction, lubrication and freezing is further complicated by abrasion of the frictional surfaces over time, and by local and large-scale variations in the salinity of the ice. To characterize friction effectively is therefore complicated [see *Hatton et al.*, 2009] for a discussion of the micromechanics of ice friction). One aim of this paper is to propose a model of sea ice friction which incorporates the effects of these separate frictional processes, while maintaining sufficient simplicity to be incorporated into sea ice dynamical models [e.g., *Hibler*, 2001; *Feltham*, 2008].

[4] The simplest model of friction is Amonton's law

$$F_t = \mu F_n, \tag{1}$$

in which F_n is the normal force, F_t is the tangential friction force, and μ is a constant coefficient of friction. This law describes dry friction. *Bowden and Hughes* [1939] proposed that the low kinetic friction coefficient they measured for ice was due to a thin water layer caused by frictional melting of the ice. *Oksanen and Keinonen* [1982] went on to produce a mathematical model of this melting which successfully predicts steady state kinetic friction measured in his experiments. Later, *Jones et al.* [1991] and *Kennedy et al.* [2000] went on to experimentally quantify the steady state kinetic friction of saline ice against itself across a range of temperatures, slip rates and nominal pressures. *Kennedy et al.* [2000] note that ice friction can be divided into three regimes: at low slip rates, friction is creep controlled; at intermediate slip rates, friction is controlled by surface fracture; and at high slip rates, friction is controlled by surface melting. Alongside this investigation of steady state friction, we and other groups have investigated the role of

[1]Rock and Ice Physics Laboratory, Department of Earth Sciences, University College London, London, UK.
[2]Centre for Polar Observation and Modelling, University College London, London, UK.
[3]British Antarctic Survey, Cambridge, UK.

0148-0227/11/2010JC006334

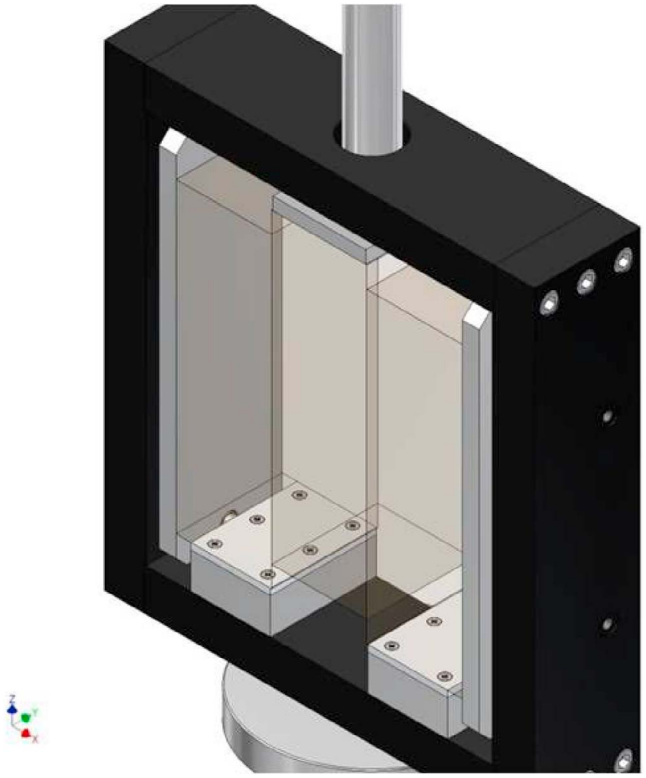

Figure 1. Schematic of experimental apparatus. The outer ice blocks are milled to dimensions 300 × 100 × 100 mm; the inner block is milled to dimensions 200 × 100 × 100 mm. The supporting frame provides a controlled, metered normal load, and the hydraulic vertical actuator drives the central ice block in shear. The entire apparatus shown is housed in a temperature-controlled environmental chamber.

surface adhesion and freezing in friction [e.g., *Maeno and Arakawa*, 2004; *Hatton et al.*, 2009]. Further complicating the picture, stick-slip behavior has been observed in multiyear sea ice friction [*Sammonds et al.*, 1998]. We note that the friction coefficient μ is often used within sea ice models as a tuning parameter [e.g., *Hopkins*, 1996] rather than treated as a known physical constant.

[5] Sea ice is deformed by ridging, rafting and in-plane sliding [*Hibler*, 2001]. Each of these processes involves frictional sliding between ice blocks. In this paper we focus on edge-edge sliding of columnar sea ice, and so the results and observations have particular significance for understanding the in-plane sliding of Arctic sea ice floes. *Kwok* [2001] shows RADARSAT images demonstrating that the Arctic sea ice cover is dominated by a few basin-scale shear zones. By analogy with faulting in the Earth's crust [*Sammonds and Rist*, 2001] we believe overall dynamics of the Arctic depend heavily on frictional sliding within these shear zones.

[6] In this work we focus on the importance of nonsteady state behavior. We present experimental data from University College London's (UCL) Ice Physics Laboratory (on the centimeter scale) and from the Hamburgische Schiffbau Versuchsanstalt (HSVA) ice tank in Hamburg, Germany (on the meter scale). This range of scales allows us to investigate the applicability of the friction model on scales beyond those for which we can control experiments, namely, Arctic floe scales. We limit our experiments to regimes in or close to the surface melting regime, over which friction can be reasonably approximated as decreasing log linearly with increasing slip rate (although *Oksanen and Keinonen* [1982] and *Kennedy et al.* [2000] propose a more complex relationship). We then note, by analogy with the rock physics literature [*Sammonds and Rist*, 2001], that memory effects in sliding may be important. The observed friction will therefore depend on the current state of the frictional contact. Again by analogy with rock physics, we propose a rate- and state-dependent model of ice friction. Such a model is physically somewhat crude (e.g., the assumption of a linearly decreasing slip rate dependence of friction), but it has the advantage of computational simplicity and direct applicability to current large-scale sea ice models. The model has been proposed recently by *Lishman et al.* [2008, 2009] and *Fortt and Schulson* [2009]. Fortt and Schulson focus on the interpreting the rate dependence of the model, while here we provide a complete set of parameter values including the state dependence. We conduct experiments with analogs in rock physics [e.g., *Dieterich*, 1978; *Ohnaka et al.*, 1987] (following the methodology of *Sammonds et al.* [2005]). Toward the end of this paper we show results of typical transient sliding experiments where our proposed rate and state model allows us to predict various aspects of transient friction which cannot be understood through a constant or rate-dependent friction model.

[7] The paper is arranged as follows. In section 2 we describe the experimental configurations used in the laboratory at UCL, and in an analogous set of experiments undertaken on a larger scale at the HSVA ice tank. In section 3 we show results from these experiments which allow us to express a log linear rate dependence of ice friction. We go on in section 4 to consider a series of experimental results based on the effects of static normal loading, by analogy with *Dieterich* [1978], which allows us to determine the state dependence of our model. We then propose a simple model for time-dependent friction in ice. In section 5 we test this model by investigating its predictions for a typical transient sliding experiment [cf. *Ohnaka et al.*, 1987] and discuss qualitatively and quantitatively the predictions of our model as compared to a constant or rate-dependent friction model. We then conclude by summarizing our research and suggesting possible applications and avenues for future work.

2. Experimental Setup

[8] The configuration of our laboratory experiments is shown in photograph and schematic in Figure 1. The experiments are in double shear configuration, in which a central slider is moved under normal load between two

Table 1. Experimental Ice Details

Location	Laboratory	Ice Tank
Ice thickness (m)	0.1	0.25
Temperature (°C)	−10	−10
Water salinity (ppt)	33	33
Bulk ice salinity (ppt)	10.8	7.3
Ice density (kg m^{-3})	930	931

Figure 2. The HSVA environmental test basin. Shear load is applied using the carriage-mounted pusher plate visible in the center of the picture. Normal load is applied using pneumatic rams mounted on the wooden frames visible in the lower left of the picture. Figure 4 shows a schematic illustration of this experimental configuration.

stationary parallel surfaces. This configuration is directly comparable to direct shear rock mechanics friction experiments [e.g., *Sammonds and Ohnaka*, 1998]. We use (as illustrated) two static cuboid blocks of columnar ice, 300 × 100 × 100 mm, and a central block 200 × 100 × 100 mm, cut from larger saline ice discs. These discs are grown in insulated cylindrical tanks at an air temperature of −10°C and with basal heating to model realistic natural sea ice growth, with typical grain dimensions 10mm in the horizontal plane and 50 mm in the vertical direction. Thin section photographs of the ice in the x–y and x–z planes are shown in Figure 3, alongside comparable photos from the tank ice (discussed below). Further details of the ice properties are given in Table 1. All experiments were conducted in a controlled environmental chamber at −10°C. All surfaces are milled to 10 μm precision immediately before experiments. The central ice block is clamped between two identical ice blocks using a metered hydraulic normal loading frame, and moved perpendicular to the normal load using a metered hydraulic actuator. Typical side loads are around 1 kN, corresponding to a normal pressure of around 50 kPa. All load cells are externally calibrated using a compression load cell (rated to ±0.1 kg) which had itself been calibrated by direct loading with free weights of known mass. Parallelism is assumed throughout. The effective friction coefficient μ is given by the direct load divided by twice the normal load (the factor of two occurs since the normal load acts on both sliding faces).

[9] This experimental configuration was used for a series of friction experiments, as discussed in section 1. Before presenting the results of these experiments, we also describe a series of friction experiments which were conducted in the HSVA Arctic Environmental Test Basin over the summer of 2008. The basin is 30 m long, 6 m wide, and 1.2 m deep, allowing experiments to be conducted on a scale of a few meters. Air temperature is controllable to a minimum of −20°C, which allows us to simulate typical Arctic conditions. An in-plane force of up to 10 kN can be applied along the length of the tank via a motorized carriage, and an in-

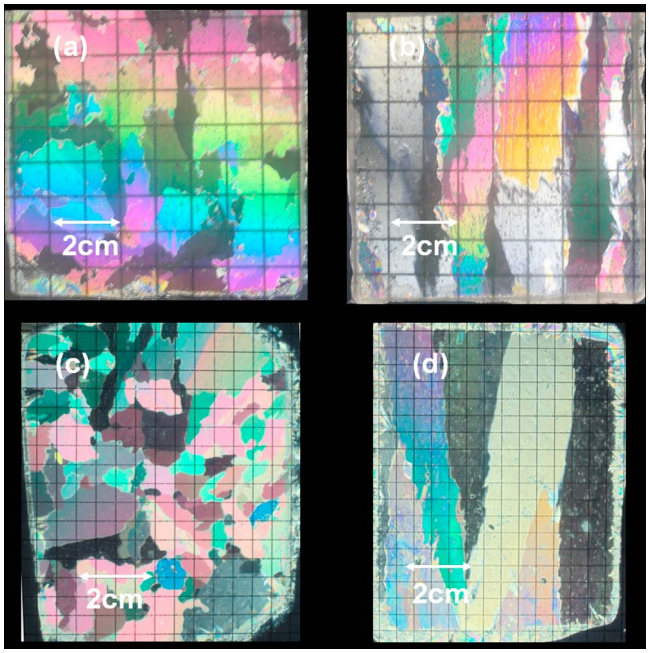

Figure 3. Thin sections of ice from (a) HSVA experiments, x-y plane; (b) HSVA experiments, x-z plane; (c) UCL experiments, x-y plane; and (d) UCL experiments, x-z plane. For the HSVA experiments the overlaid grid is marked out in centimeter squares and for the UCL experiments it is marked out in half centimeter squares.

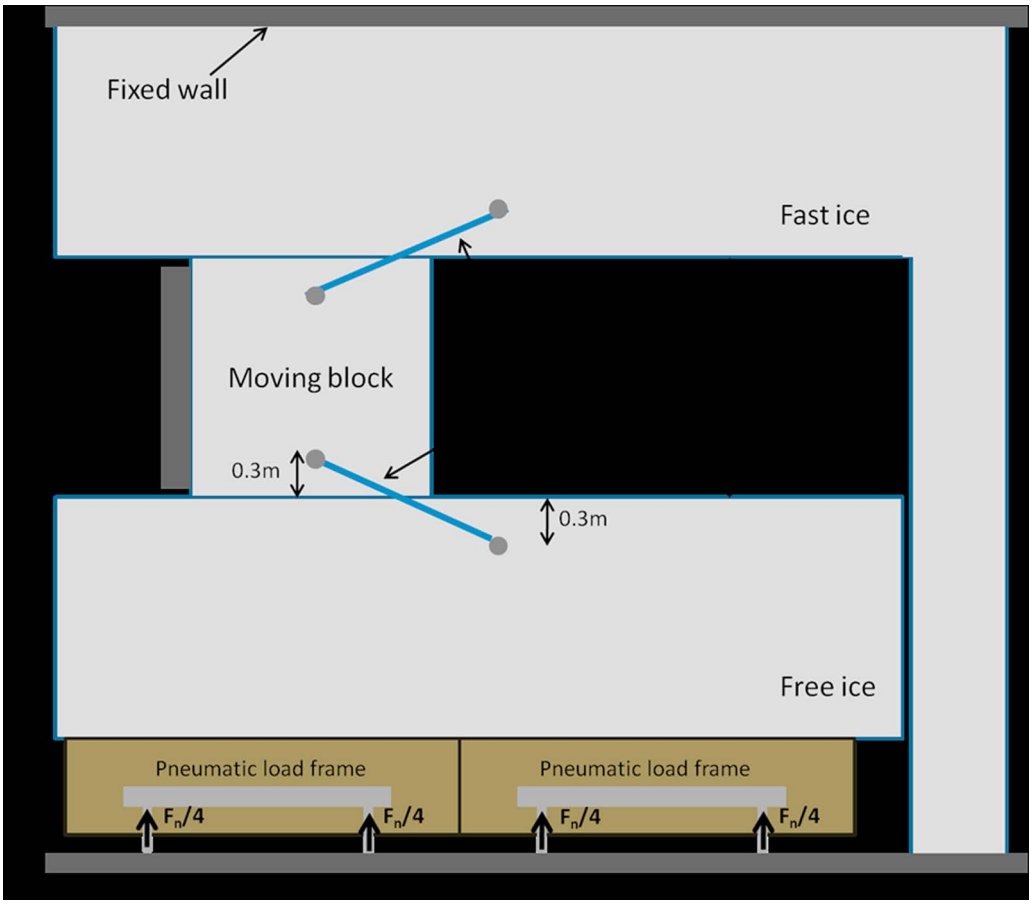

Figure 4. Schematic of ice tank experiments. The moving central ice block has dimensions 2 m × 2 m × 0.25 m.

plane force of up to 15 kN can be applied across the width of the tank by pneumatic side-loading frames. Figure 2 gives a sense of the configuration and scale of the test basin. Level ice was grown from saline water (33 ppt) at −10°C over a period of two weeks, and the relevant ice properties are shown in Table 1. Again, thin section photographs are shown in Figure 3; typical grain sizes are 20 mm in the horizontal direction and 50 mm in the vertical. The sliding interfaces were >1 m from the tank walls, and no temperature gradient was observed in the tank, and so we assume the ice forms a homogeneous sheet and the thin sections shown are representative throughout. The ice was cut using handsaws, giving a rough surface with visible asperities and notches on the scale of 1 mm. Each time the ice was recut, we conducted an unmetered slide to reduce the roughness to post-sliding levels (however, the roughness of the ice surface was still higher for the ice tank tests than for the laboratory tests). A further possible variation between ice tank and laboratory experiments is in brine drainage. In the ice tank the brine drainage is expected to model a natural environment, since the ice is floating in its typical orientation in saline water. In contrast, in the laboratory the ice is handled in air, and reoriented for testing so that the sliding contact is perpendicular to the columnar growth direction, and this leads to brine drainage.

[10] A plan drawing of our experimental setup is shown in Figure 4. A 2 m square floating ice block, 25 cm thick, was subjected to loading between two parallel ice sheets. Typical normal (side) loads were 5 kN, corresponding to a normal pressure of 10 kPa. The floating block was pushed along the length of the tank by a pusher attached to the mechanical carriage. The speed is selected by a relatively crude control on the carriage but measured by accurate displacement transducers. The load required to move the block was measured by two shear load cells supporting the pushing plate. All load cells were externally calibrated as above. Slip displacement was measured using two free pivoting displacement transducers as shown in the diagram, and this arrangement was chosen to allow the maximum total slip distance for our equipment. The displacement transducers were pinned 30 cm from the sliding contact on both sides, so all displacements should be seen as bulk rather than local. The use of two displacement transducers on either side of the tank allows us to detect variations from parallelism (since variations between the recorded slip on each transducer must be caused by motion in the y direction in Figure 4). These are never greater than 10 mm and so we assume parallelism and a continuous transverse contact throughout. In both the ice tank and laboratory experiments we assume a constant nominal contact area, as the effects of small changes in contact area (e.g., due to melting in the ice tank) are assumed to be of lower order than the frictional variations of interest to the present work. The ice tank experiments occurred up to 4 h after cutting the ice, and

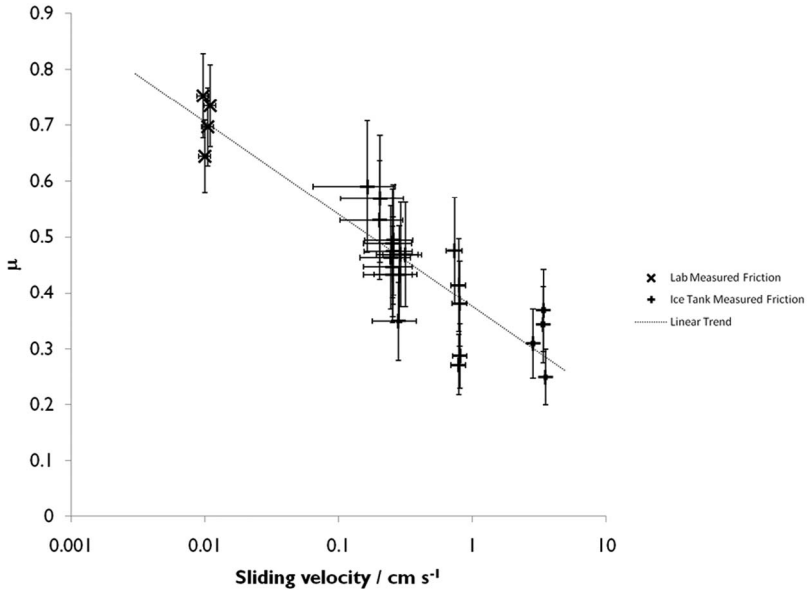

Figure 5. Experimentally determined rate dependence of sea ice friction. The crosses, at a sliding speed around 0.1 mm s^{-1}, are from laboratory experiments. The pluses, at higher speeds, are from ice tank experiments. The horizontal error bars represent variations in the pusher speed due to stick-slip behavior, while the vertical error bars represent variations in the normal load.

surface properties may have changed over this time, due to melting and abrasion. However, frictional behavior did not clearly correlate with the time since cutting.

3. Rate Dependence and Hold Time Dependence

[11] To investigate the rate dependence of ice friction, tests were run in the laboratory at 0.1 mm s^{-1}, and in the ice tank at three different carriage speeds: 3, 8, and 30 mm s^{-1}. The laboratory-measured rate dependence of friction is plotted (crosses) alongside the ice tank results (pluses) in Figure 5. The vertical error bars represent variations in the side loads due to inconsistent hydraulic pressure, while the horizontal error bars represent uncertainties in the slip rate due to occasional stick-slip sliding. As explained above, our laboratory experiments and ice tank experiments are not perfect analogs, due to variations in, e.g., brine drainage and surface roughness. However, we note that a linear relationship between μ and ln(slip rate) appears to hold, such that

$$\mu = \mu_0 + C_1 \ln\left(\frac{V}{V_*}\right), \tag{2}$$

where V_* is a characteristic velocity for dimensional consistency, chosen here as 10^{-5} m s^{-1}. Here μ_0 and C_1 are empirically determined constants; we find that $\mu_0 = 0.872$ and $C_1 = -0.072$ (with coefficient of determination $R^2 = 0.82$). We note that this value is in good agreement with *Fortt and Schulson* [2009], who find a value of -0.10 ± 0.6 for acceleration, -0.16 ± 0.2 for deceleration, and -0.12 at constant velocity all at comparable slip rates (see their Tables 2 and 3). These values also all come from equivalent experiments conducted on one scale. Clearly the parameter is not yet well constrained, and any of these numbers could be substituted for our C_1 (and later $A - B$, see section 4). We note here that *Kennedy et al.* [2000] and *Fortt and Schulson* [2009] both show evidence of a nonmonotonic relationship between slip rate and steady state friction, such that friction increases with increasing slip rate up to speeds around 10^{-5} m s^{-1}. Here we focus on higher slip rates and so consider only the regime where friction can be considered to decrease linearly with logarithmically increasing slip rate [see *Fortt and Schulson*, 2009, Figure 1].

[12] To investigate the state dependence of friction, we follow the methodology of *Dieterich* [1978] and *Ruina* [1983] in determining the effects of static "hold" periods on subsequent friction: the central sliding block was moved; then held still under normal load for a given period (the hold time); then moved again at the original speed. In the laboratory we used a speed of 0.1 mm s^{-1} throughout, and hold times of 1, 10, 100, and 1000 s. In the ice tank we used a speed of 8 mm s^{-1} throughout, and hold times of 10, 100, and 1000 s. The difference in speeds was due to the experimental equipment available; the laboratory actuator and ice tank carriage do not have an overlapping velocity region in which reasonable experiments can be conducted. On resumption of motion we expect friction to rise above the steady state value temporarily due to low lubrication and breaking of freeze bonds. The maximum (or "spike") value of the friction coefficient μ_s is shown for these experiments

Table 2. Empirically Determined Parameter Values of a Single-State-Variable Constitutive Law

Parameter	Value
μ_0	0.872
A	0.310
B	0.382

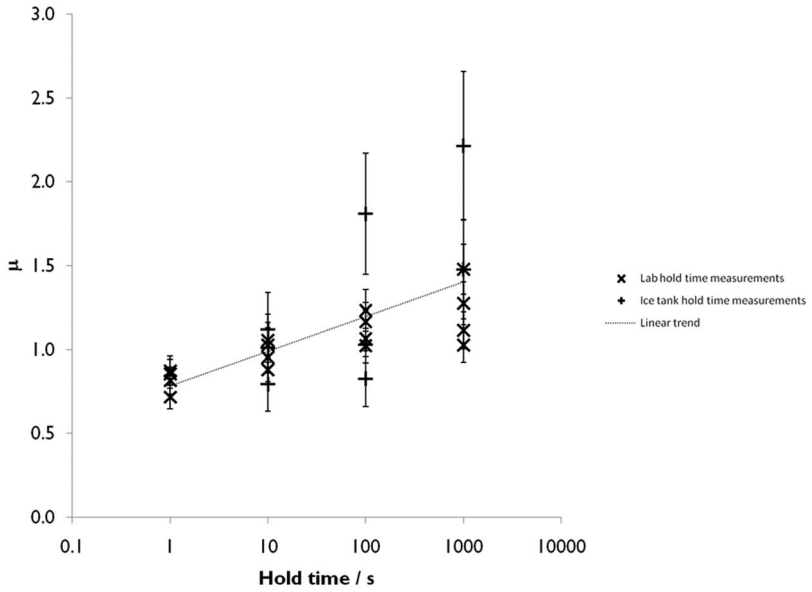

Figure 6. Experimental determination of the effects of static contact on the friction spike on resumption of motion. Crosses show laboratory data, while pluses show ice tank data. The dotted line shows a LMS linear fit to the data.

in Figure 6. As expected, the force required to resume movement increases with increasing hold time, hence the positive slope of the least mean squares (LMS) fit overlaid on the data points. This fit has coefficient of determination $R^2 = 0.407$ (this improves to 0.566 if the two apparently outlying high results are eliminated). We note here that we only consider hold times up to 1000 s (~17 min); *Fortt and Schulson* [2007] consider experiments on fresh ice with hold times of 20 min, 24 h, and 10 days, and find little evidence of further hold time strengthening. The results here should therefore be applied to relatively dynamic situations and not expected to govern long-term (i.e., >1 h) freeze bonding. The quantitative results from these experiments can then be combined into a single rate and state friction law, which we discuss in section 4.

4. Proposed Rate and State Model

[13] Following *Gu et al.* [1984], we propose that the experimental data above can be combined to produce an empirical fit to a single-state-variable constitutive law. We introduce θ as our state variable, and the time-dependent evolution of θ accounts for the slip history. The model has the form

$$\mu = \mu_0 + \theta + A \ln \frac{V}{V_*} \tag{3a}$$

$$\frac{d\theta}{dt} = -\frac{V}{L}\left(\theta + B \ln \frac{V}{V_*}\right). \tag{3b}$$

[14] The effective friction μ of equation (3a) is made up of three parts: a constant term μ_0, a rate-dependent term A *ln* V/V_*, and a state dependence θ, which itself is controlled by the dynamics of equation (3b). Note that this set of equations only models static hold dependence when coupled with a pushing force of finite stiffness. See *Ruina* [1983] for a discussion of this point and the merits of static hold experiments). We know already from section 3 that $\mu_0 = 0.872$ and the steady state rate dependence, $(B–A) = -C_1 = 0.072$ [see *Gu et al.*, 1984]. L is a characteristic slip length given by the distance over which the friction decays from its peak to $\mu_{ss} + (1/e)(\mu_{peak} - \mu_{ss})$ (i.e., the frictional peak above steady state has reduced to a factor of $1/e$ of its original value). L is found for our laboratory experiments to be 0.2 mm [see, e.g., *Ruina*, 1983]; this value is also comparable to that of *Fortt and Schulson* [2009], whose Figure 4 shows various slip displacements in the region of 0.2 mm) and for the ice tank experiments to be 5 mm [*Lishman et al.*, 2009]. We discuss this variation of critical slip displacement below. To determine A (and hence B) for our laboratory experiments we combine the above model with a spring slider model for the pushing force and model numerically according to [cf. *Ruina*, 1983]

$$F = k\left(x_p - x_b\right), \tag{4a}$$

$$V = V_* e^{\left(\frac{F}{\sigma} - \mu_0 - \theta\right)/A}, \tag{4b}$$

$$\theta_1 = -\frac{V}{L}\left(\theta + B \ln \frac{V}{V_*}\right). \tag{4c}$$

For the spring stiffness k we use a laboratory apparatus value of 20 MN m^{-1}, and a calculated ice tank apparatus value of 2 MN m^{-1} [*Lishman et al.*, 2009]. The pusher position x_p is modeled as an appropriate profile in time (e.g., for hold time experiments, movement followed by

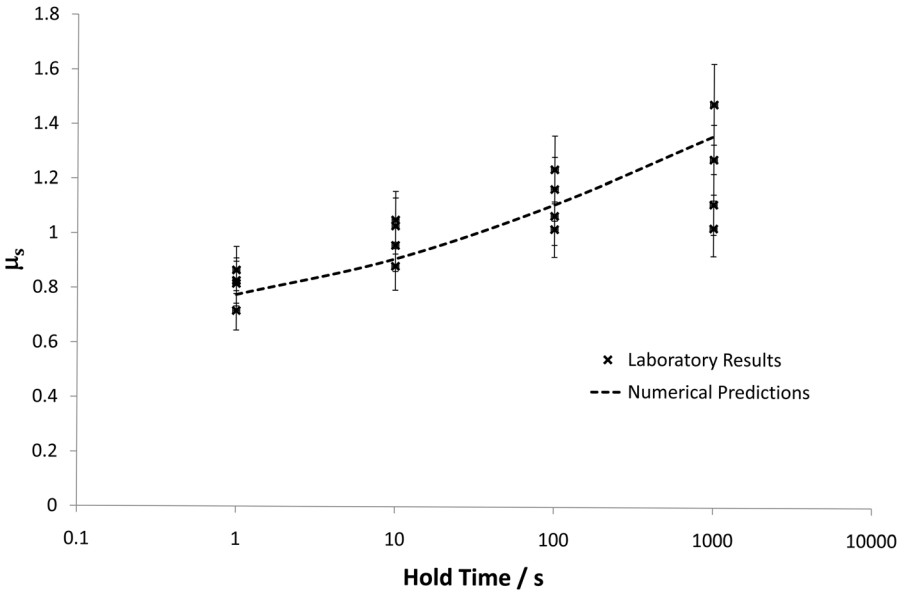

Figure 7a. Comparison of laboratory hold time data to the proposed rate and state model, with a critical slip displacement d of 0.2 mm.

pause followed by movement). V then gives the block speed and the force (and hence friction) can then be calculated numerically over the pusher position profile. We typically use a time step of 1 ms. Our observed state dependence is well modeled by (4) when $A = 0.310$ and $B = 0.382$.

[15] The fit of this model to our experiments is shown for the laboratory data in Figure 7a and to the ice tank data in Figure 7b. Note here that the empirical parameter values of Table 2 describe the model under the conditions of our specific experimental configuration (−10°C, 33 ppt water salinity). Note also that the numerical results presented in Figures 7a and 7b allow for the variation in observed critical slip displacement between our laboratory and ice tank experiments, as discussed below.

5. Model Predictions of Irregular Sliding Cycles

[16] The experimental results for hold times provide a useful way to determine empirically the coefficients of a proposed rate and state friction model. However, in order to be useful, such a model should provide improved estimates of friction over a range of sea ice dynamics, rather than just

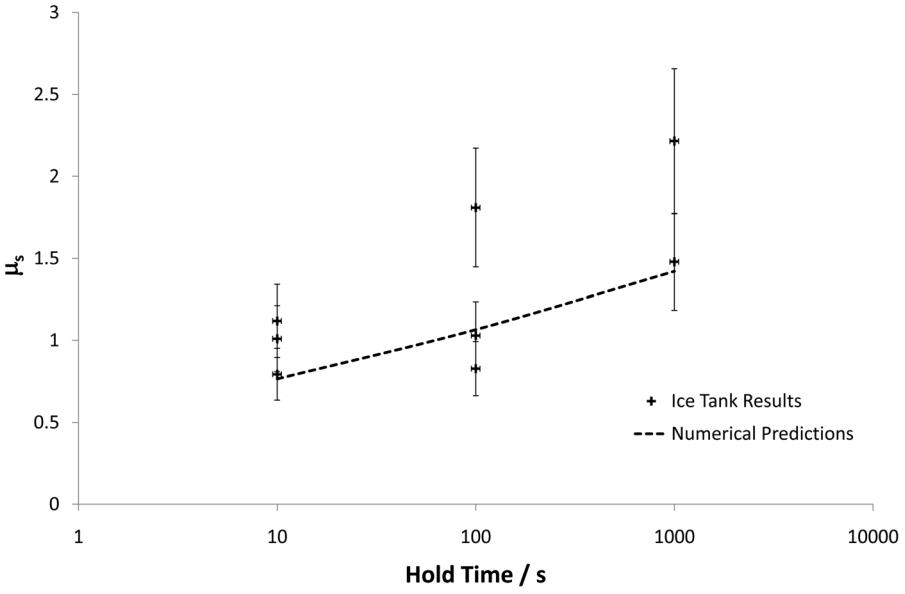

Figure 7b. Comparison of ice tank hold time data to the proposed rate and state model, with a critical slip displacement d of 5 mm.

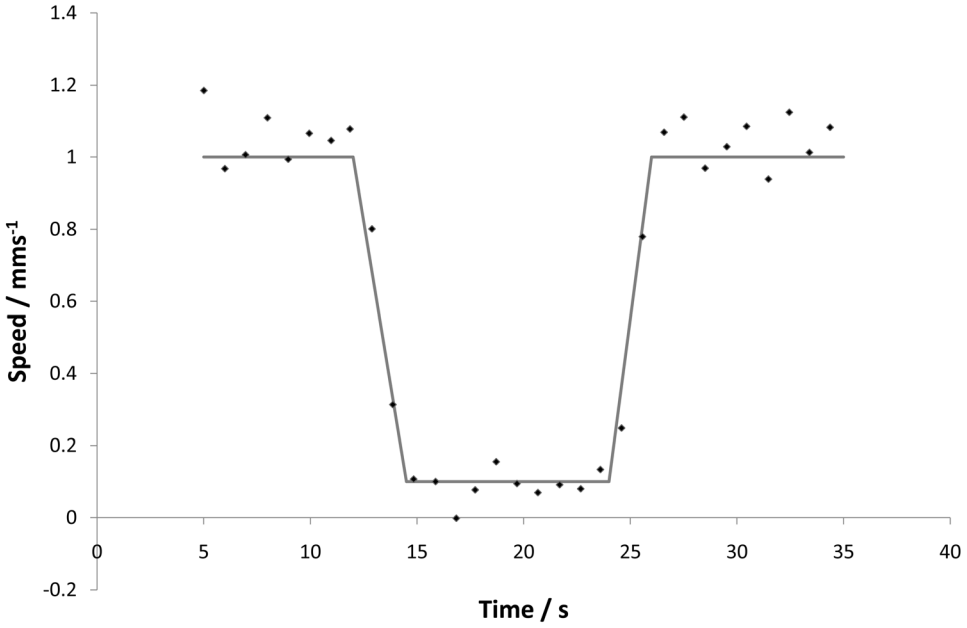

Figure 8a. A typical nonsteady state cycle, showing the pusher speed as a function of time. The diamonds show observations from a typical experimental cycle, while the solid line shows the numerical approximation used. Friction results for this cycle are shown in Figures 8b and 8c.

static loading and steady state motion. Here we test the predictions of the model over a cycle of acceleration and deceleration, and compare these predictions to those of a constant friction coefficient [cf. *Ohnaka et al.*, 1987]. The experiments in this section were conducted in the laboratory.

[17] The velocity cycle in question is shown as a function of time in Figure 8a, with the experimentally measured speeds shown as a series of diamonds, and an idealized version used for numerical convenience marked as a solid line. Figure 8b then shows the predicted friction evolution as a function of displacement; the solid lines show experimental measurements, while the dashed line shows numerical predictions. Figure 8c shows a comparison of one single cycle to our model. Qualitatively, the model predicts well the positive spike in friction on acceleration, as well as the evolutions to steady state, while overestimating the negative

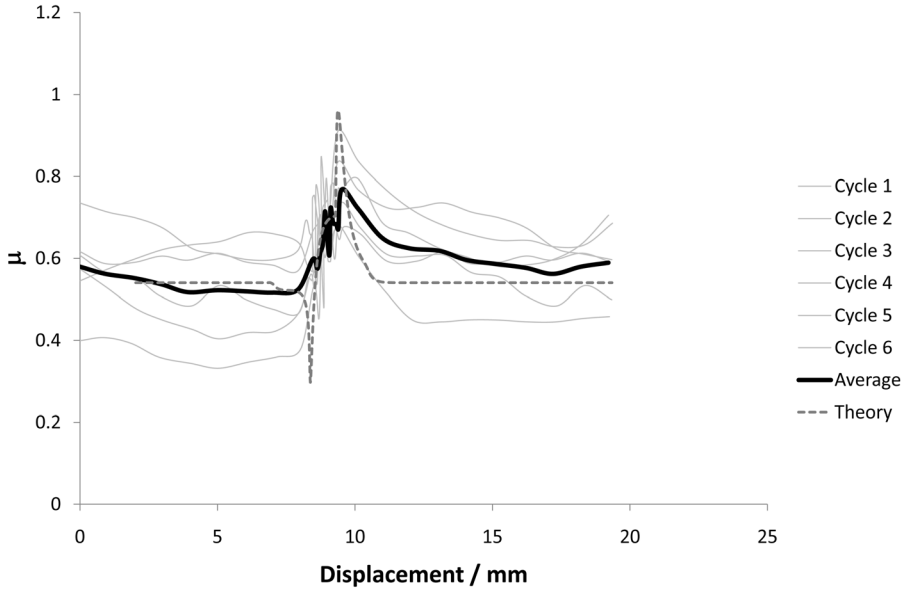

Figure 8b. Transient friction with varying speed (the speed cycle is shown in Figure 8a and the friction is plotted here as a function of displacement). The thin lines show results for six separate experiments, the bold line shows the average of these experiments, and the dashed line shows the prediction of our rate and state model for the given cycle.

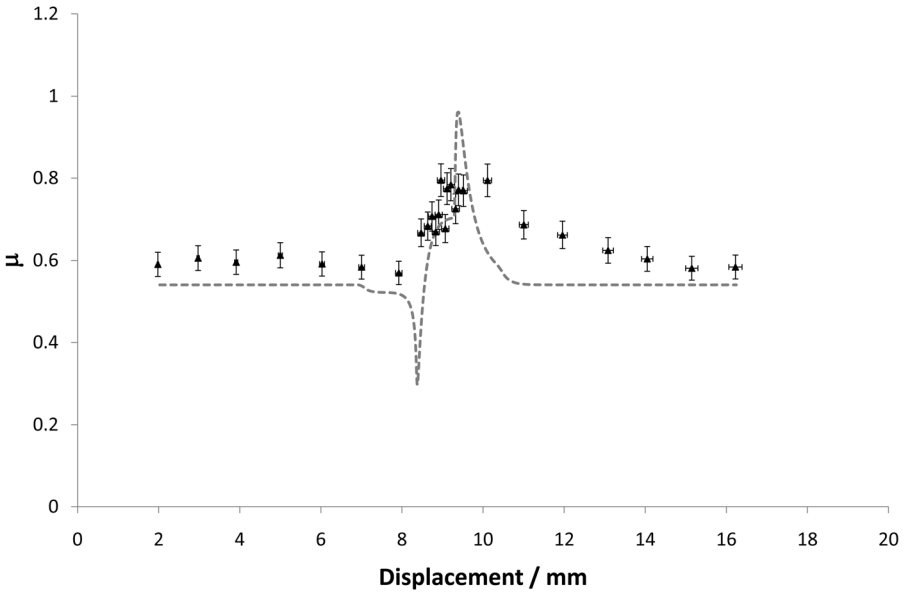

Figure 8c. Transient friction with varying speed (the speed cycle is shown in Figure 8a and the friction is plotted here as a function of displacement). The dashed line shows our numerical model, while the triangles indicate experimental values, with vertical error bars representing uncertainty in the side load measurement.

spike in friction on deceleration. In order to quantitatively assess the merits of a rate and state model, we compare it to a constant friction coefficient. We calculate the Mean Squared Error (MSE) between each of the friction models and experiment, and find that for a constant friction model the MSE is 0.027; for a rate-dependent model it is 0.014; and for a rate- and state-dependent model 0.012.

[18] Figure 9a shows a different slip rate cycle (speed as a function of time), comparable to Figure 8a. Figure 9b shows a comparison of our model and experimental data, here plotted with friction as a function of slip rate. A constant friction coefficient would be represented by a horizontal line on this graph, while a simple rate-dependent model would show a monotonic decrease in friction coefficient with increasing slip rate. Qualitatively here the rate and state

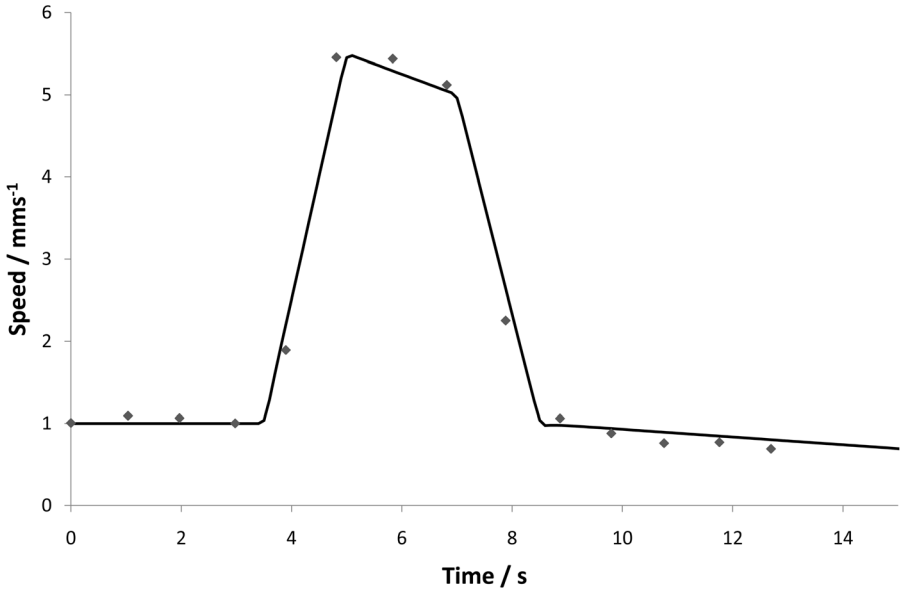

Figure 9a. A typical nonsteady state cycle, showing the pusher speed as a function of time. The diamonds show observations from a typical experimental cycle, while the solid line shows the numerical approximation used. Friction results for this cycle are shown in Figure 8b.

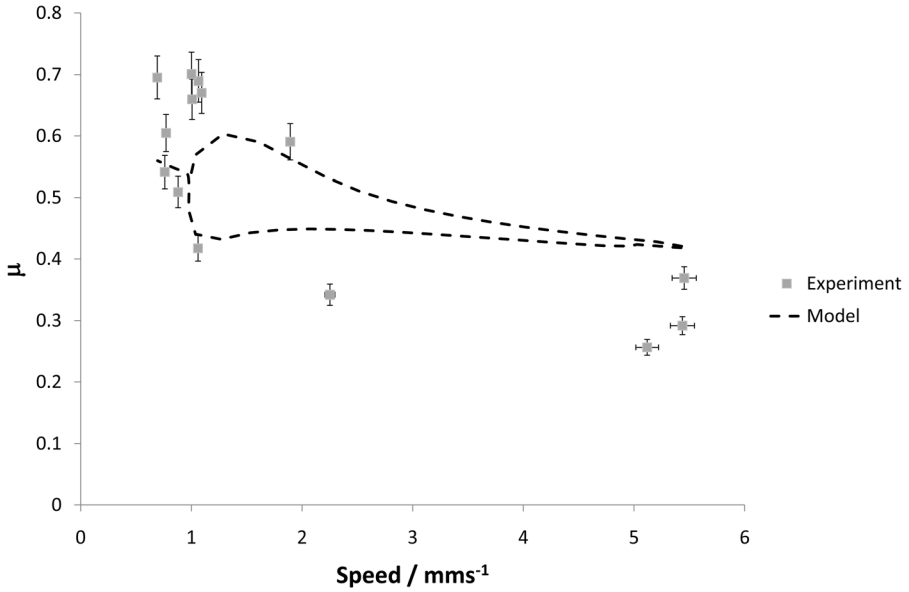

Figure 9b. Transient friction with varying speed (the speed cycle is shown in Figure 8a and the friction is plotted here as a function of displacement). The dashed line shows our numerical model, while the squares indicate experimental values, with vertical error bars representing uncertainty in the side load measurement.

model predicts the observed hysteretic cycle, with friction increasing on initial acceleration before decreasing, and vice versa. Quantitatively we find the MSE to be 0.031 for a constant friction coefficient (chosen as the average friction over the cycle); 0.014 for a rate-dependent friction coefficient; and 0.012 for a rate and state model.

6. Discussion and Conclusions

[19] We have presented experimental results showing transient behavior in ice friction on the laboratory scale and the ice tank scale. We have focused in particular on the macroscopic properties of slip rate and slip history. We have suggested that some aspects of the observed frictional behavior are not well predicted unless slip history is taken into account. We have proposed that transients in ice friction may be well predicted by a single-state-variable rate and state model, with $\mu_0 = 0.872$, $A = 0.310$, and $B = 0.382$. This model is somewhat simplistic, but this simplicity is also an advantage, as it allows us to describe friction using only three parameters (μ_0, A, and B in equations (3a) and (3b)) and allows for easy computation. The rate and state model is shown in a case study to predict transient friction significantly better than a constant model of ice friction.

[20] The rate dependence of ice friction has been studied before, notably by *Jones et al.* [1991] and *Kennedy et al.* [2000]. These studies found the same decrease in friction with slip rate as in this study. Their overall friction coefficient was somewhat lower (around 0.2) and we cannot fully explain this discrepancy. However, one possibility is that the difference is due to differences in surface preparation, since *Kennedy et al.* used a microtome to smooth surfaces to micron precision (see *Gu et al.* [1984], *Fortt and Schulson* [2009], and *Hatton et al.* [2009] for a discussion of the importance of surface characteristics in predicting rock friction and ice friction). Typical natural sea ice is likely to have initially rough sliding surfaces, which are then abraded to smoothness and lubricated by gouge over the course of sliding; this is quantified by *Fortt and Schulson* [2009]. Our results are in good agreement with the overall review of steady state friction presented by *Maeno et al.* [2003], and we note from Maeno et al. that there are wide variations in measurements of steady state ice friction. We note also that *Rist* [1997] proposes a nonlinear relationship between steady state shear stress and normal stress in fresh ice, and that we have not investigated how varying normal stress affects our results. Current discrete element studies of sea ice floe interaction use values of μ in the range 0.2–0.8 [e.g., *Hopkins*, 1996], which accords well with our results.

[21] To give a sense of the importance of the variable parameters A, B, and L, we present in the sensitivity plots of Figures 10a–10c, showing the effect of varying A (Figure 10a), (B–A) (Figure 10b), and L (Figure 10c) by 20% up or down. We see that such a variation in A or L has a slight qualitative effect on the shape of the curve, while varying (B–A) mainly affects the vertical position of the entire curve (which would also occur with variations in μ_0). It is also worth noting that the numerical results always have a concave shape, where the change in friction at higher speeds is small, and that this does not appear a good match for the experimental data presented in Figure 9b. This may hint at the limitations of the simple model used in this paper, and in future work we hope to address this.

[22] One key parameter in the proposed model is the critical slip displacement L. If this parameter is known then the proposed rate and state model provides a useful way to predict transient effects in ice friction, as shown in section 5. However, our comparison of laboratory and ice tank results

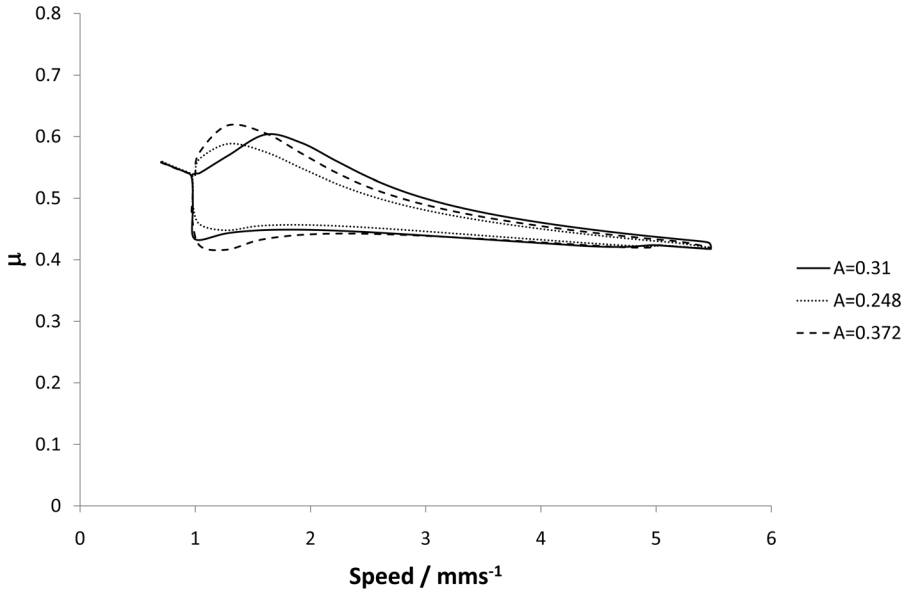

Figure 10a. Sensitivity test on the parameter A. The modeled data of Figure 8b (corresponding to the slip rate profile of Figure 8a) is replotted for $A = 0.31$ (as in Figure 8b), $A = 0.31 \times 0.8$, and $A = 0.31 \times 1.2$.

shows that the critical slip displacement cannot be considered a material constant for ice but varies with scale. Indeed, looking at the data presented by *Fortt and Schulson* [2009, Figure 3], it is not clear that L can be considered a constant across various rate changes in ice friction. We therefore propose that in order for our results to be applicable across scales a further investigation into the behavior of the parameter L is required.

[23] The advantage of laboratory and ice tank experiments is that inputs and environmental conditions can be closely controlled to highlight important relationships and provide insights into behavior. We note, though, that the experiments described here are only an approximation to the dynamic Arctic environment in which we wish to predict sea ice behavior. Out-of-plane behavior, jostling, and ocean waves may decrease the effects of slip history, while local variations in temperature and salinity may lead to variations in the parameters of our model. We also note that the analogy between rock friction and ice friction is imperfect. In particular, under sufficient static contact refreezing of asperities will dominate friction, and eventually the contact strength will asymptotically approach the shear strength of

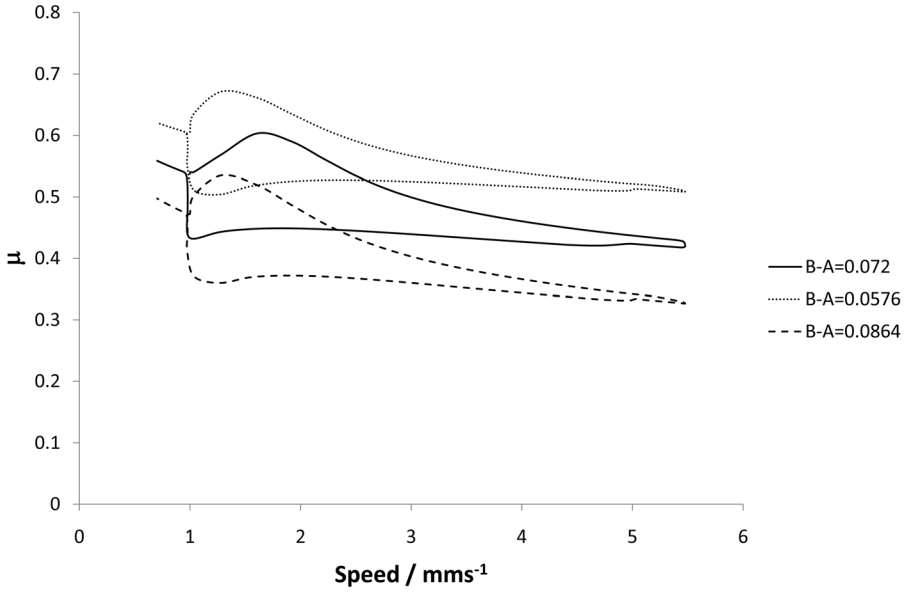

Figure 10b. Sensitivity test on $B–A$. The modeled data of Figure 8b is replotted for $(B–A) = 0.072$ (as in Figure 8b), $(B–A) = 0.072 \times 0.8$, and $(B–A) = 0.072 \times 1.2$.

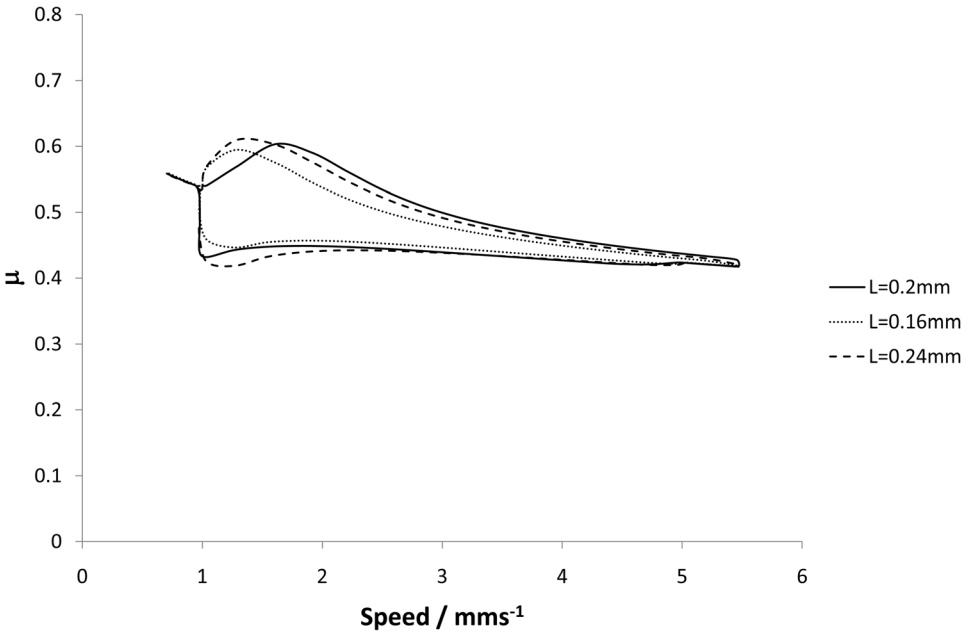

Figure 10c. Sensitivity test on L. The modeled data of Figure 8b is replotted for L = 0.2 mm (as in Figure 8b), L = 1.6 mm, and L = 2.4 mm.

level sea ice. In our ice tank experiments we found that with a hold time of several hours the loads required to initiate movement of the ice were too high for our equipment. The results in this paper are limited to slip rates above 10^{-4} m s^{-1}, and hold times up to 20 min. It seems possible that by amalgamating the present work with the results of *Fortt and Schulson* [2007, 2009] the range of applicability could be extended; this would need to be tested experimentally.

[24] In this work we have focused on a single parallel pair of sliding contacts as a simple way to understand friction behavior. However, the ultimate aim of this work is to better predict the ensemble behavior of floes of sea ice. In a future paper, therefore, we plan to use a discrete element model of ice dynamics [*Hopkins*, 1996] to investigate how a rate and state model of ice friction affects ice dynamics across, e.g., a simple tessellation of discrete, diamond-shaped floes, when compared to simpler friction models. Further work might also allow us to reconcile the results of this study with insights into the mechanics of stick-slip behavior [*Sammonds et al.*, 2005] and the freeze bonding of asperities [see, e.g., *Repetto-Llamazares et al.*, 2009]. With the exception of the critical slip displacement, our results are consistent across the laboratory and ice tank scales investigated. Further work may allow us to understand scale effects in the critical slip displacement, which would give a fuller understanding of how laboratory friction results can be scaled to predict Arctic basin-scale dynamics.

[25] **Acknowledgments.** This work was funded by the National Environmental Research Council. The ice tank work was supported by the European Community's Sixth Framework Programme through the grant to the budget of the Integrated Infrastructure Initiative HYDRALAB III, contract 022441(RII3). The authors would like to thank the Hamburg Ship Model Basin (HSVA), especially the ice tank crew, for the hospitality and technical and scientific support. D.F. would like to thank the Leverhulme Trust for the award of a prize that made his participation in the HSVA experiments possible. The authors would like to thank Steve Boon, Eleanor Bailey, Adrian Turner, and Alex Wilchinsky for their contributions to the ice tank work.

References

Bowden, F. P., and T. P. Hughes (1939), The mechanism of sliding on ice and snow, *Proc. R. Soc. A*, *172*, 280–298, doi:10.1098/rspa.1939.0104.

Dieterich, J. H. (1978), Time-dependent friction and the mechanics of stick-slip, *Pure Appl. Geophys.*, *116*, 790–806, doi:10.1007/BF00876539.

Feltham, D. L. (2008), Sea ice rheology, *Annu. Rev. Fluid Mech.*, *40*, 91–112, doi:10.1146/annurev.fluid.40.111406.102151.

Fortt, A. L., and E. M. Schulson (2007), The resistance to sliding along Coulombic shear faults in ice, *Acta Mater.*, *55*, 2253–2264, doi:10.1016/j.actamat.2006.11.022.

Fortt, A. L., and E. M. Schulson (2009), Velocity dependent friction on Coulombic shear faults in ice, *Acta Mater.*, *57*, 4382–4390, doi:10.1016/j.actamat.2009.06.001.

Gu, J., J. R. Rice, A. L. Ruina, and S. T. Tse (1984), Slip motion and the stability of a single degree of freedom elastic system with rate and state dependent friction, *J. Mech. Phys. Solids*, *32*, 167–196, doi:10.1016/0022-5096(84)90007-3.

Hatton, D. C., P. R. Sammonds, and D. L. Feltham (2009), Ice internal friction: Standard theoretical perspectives on friction codified, adapted for the unusual rheology of ice, and unified, *Philos. Mag.*, *89*, 2771–2799, doi:10.1080/14786430903113769.

Hibler, W. D. (2001), Sea ice fracturing on the large scale, *Eng. Fract. Mech.*, *68*, 2013–2043, doi:10.1016/S0013-7944(01)00035-2.

Hopkins, M. A. (1996), On the mesoscale interaction of lead ice and floes, *J. Geophys. Res.*, *101*, 18,315–18,326, doi:10.1029/96JC01689.

Hopkins, M. A., W. D. Hibler, and G. M. Flato (1991), On the numerical simulation of the sea ice ridging process, *J. Geophys. Res.*, *96*, 4809–4820, doi:10.1029/90JC02375.

Jones, D. E., F. E. Kennedy, and E. M. Schulson (1991), The kinetic friction of saline ice against itself at low sliding velocities, *Ann. Glaciol.*, *15*, 242–246.

Kennedy, F. E., D. E. Jones, and E. M. Schulson (2000), The friction of ice on ice at low sliding velocities, *Philos. Mag. A*, *80*, 1093–1110, doi:10.1080/01418610008212103.

Kwok, R. (2001), Deformation of the Arctic Ocean sea ice cover between November 1996 and April 1997: A qualitative survey, in *IUTAM Symposium on Scaling Laws in Ice Mechanics and Ice Dynamics*, edited by J. P. Dempsey and H. H. Shen, pp. 315–322, Kluwer Acad., Dordrecht, Netherlands.

Lishman, B., P. R. Sammonds, and D. L. Feltham (2008), Rate- and state-dependence of ice-ice friction in sea ice, *Eos Trans. AGU*, *89*(53), Fall Meet. Suppl., Abstract U13C–0062.

Lishman, B., P. R. Sammonds, D. L. Feltham, and A. Wilchinsky (2009), The rate- and state- dependence of sea ice friction, paper presented at 20th International Conference on Port and Ocean Engineering Under Arctic Conditions, Luleå Univ. of Technol., Luleå, Sweden.

Maeno, N., and M. Arakawa (2004), Adhesion shear theory of ice friction at low sliding velocities, combined with ice sintering, *J. Appl. Phys.*, *95*, 134–139, doi:10.1063/1.1633654.

Maeno, N., M. Arakawa, A. Yasutome, N. Mizukami, and S. Kanazawa (2003), Ice-ice friction measurements, and water lubrication and adhesion-shear mechanisms, *Can. J. Phys.*, *81*, 241–249, doi:10.1139/p03-023.

Ohnaka, M., Y. Kuwahara, and K. Yamamoto (1987), Constitutive relations between dynamic physical parameters near a tip of the propagating slip zone during stick-slip failure, *Tectonophysics*, *144*, 109–125, doi:10.1016/0040-1951(87)90011-4.

Oksanen, P., and J. Keinonen (1982), The mechanism of friction of ice, *Wear*, *78*, 315–324, doi:10.1016/0043-1648(82)90242-3.

Repetto-Llamazares, A. H. V., K. V. Hoyland, K. U. Evers, and P. Jochmann (2009), Preliminary results of freeze bond strength and initial freezing experiments, paper presented at 20th International Conference on Port and Ocean Engineering Under Arctic Conditions, Luleå Univ. of Technol., Luleå, Sweden.

Rist, M. A. (1997), High-stress ice fracture and friction, *J. Phys. Chem. B*, *101*, 6263–6266, doi:10.1021/jp963175x.

Ruina, A. (1983), Slip instability and state variable friction laws, *J. Geophys. Res.*, *88*, 10,359–10,370, doi:10.1029/JB088iB12p10359.

Sammonds, P. R., and M. Ohnaka (1998), Evolution of Microseismicity during frictional sliding, *Geophys. Res. Lett.*, *25*, 699–702, doi:10.1029/98GL00226.

Sammonds, P. R., and M. A. Rist (2001), Sea ice fracture and friction, in *Scaling Laws in Ice Mechanics and Ice Dynamics*, edited by J. P. Dempsey and H. H. Shen, pp. 183–194, Kluwer Acad., Dordrecht, Netherlands.

Sammonds, P. R., S. A. F. Murrell, and M. A. Rist (1998), Fracture of multiyear sea ice, *J. Geophys. Res.*, *103*, 21,795–21,815.

Sammonds, P. R., D. Hatton, D. L. Feltham, and P. D. Taylor (2005), Experimental study of sliding friction and stick-slip on faults in floating ice sheets, paper presented at 18th International Conference on Port and Ocean Engineering Under Arctic Conditions, Clarkson Univ., Potsdam, N. Y.

Weiss, J., E. M. Schulson, and H. L. Stern (2007), Sea ice rheology from in-situ, satellite and laboratory observations: Fracture and friction, *Earth Planet. Sci. Lett.*, *255*, 1–8, doi:10.1016/j.epsl.2006.11.033.

Wilchinsky, A. V., D. L. Feltham, and P. A. Miller (2006), A multithickness sea ice model accounting for sliding friction, *J. Phys. Oceanogr.*, *36*, 1719–1738, doi:10.1175/JPO2937.1.

D. Feltham, Centre for Polar Observation and Modelling, University College London, Gower Street, London WC1E 6BT, UK.

B. Lishman and P. Sammonds, Rock and Ice Physics Laboratory, Department of Earth Sciences, University College London, Gower Street, London WC1E 6BT, UK. (b.lishman@ucl.ac.uk)